Facile synthesis of novel blue light and large Stoke shift emitting tetradentate polyazines based on imidazo[1,5-a]pyridine – Part 2

Facile synthesis of novel blue light and large Stoke shift emitting tetradentate polyazines based on imidazo[1,5-a]pyridine – Part 2

G. Volpi, C. Garino*, E. Priola, E. Diana, R. Gobetto, R. Buscaino, G. Viscardi, C. Barolo

Dipartimento di Chimica, NIS Interdepartmental Centre, Università di Torino, Via Pietro Giuria 7, 10125, Torino, Italy. Fax: +39 011 670 7855; Tel: +39 011 670 7943; E-mail: claudio.garino@unito.it
* corresponding author

Keywords: imidazo[1,5-a]pyridine, multidentate ligand, large Stokes' shift, blue emitter, down-converter

Abstract

A series of new imidazo[1,5-a]pyridines was obtained through a facile multiple condensation procedure, involving the reaction of two methanamine and several largely available and inexpensive di- and tricarboxylic acids. Such poliazine products show different and tuneable coordination motifs suitable for mono-, di-, and tritopic coordination sites. Furthermore they display interesting optical properties: tuneable luminescence, significant quantum yields, large Stokes' shifts and strong halochromic effects, enabling their technological application.

1. Introduction

In the last years, imidazo[1,5-a]pyridines have attracted a growing attention due to their unique chemical, optical and biological properties. This class of aromatic heterocyclic compounds has potential in several research areas, from material science to pharmaceutical fields. Indeed, imidazo[1,5-a]pyridines are employed as precursors of N-heterocyclic carbenes [1–4], as ligands in coordination chemistry [5–13] and as pH-probes [14–16]. They also represent an interesting class of organic materials for fluorescence microscopy and for down-shifting luminescent layers both in lighting and photovoltaic technologies [5,15–18]. Furthermore, the imidazo[1,5-a]pyridine core is present in several drug relevant molecules and biologically active agents such as: HIV-protease inhibitors [19], cardiotonic agents [20], aromatase inhibitors in oestrogen dependent diseases [21], thromboxane A_2 synthetase inhibitors [22], RORc inverse agonists in inflammatory diseases [23], 5-HT4 receptor partial agonists in Alzheimer's disease [24] and antitumor agents [25].

From the synthetic point of view, the imidazo[1,5-a]pyridine nucleus can be achieved by the Vilsmeier-type cyclizations and their variants, with modest efficiency [26–28], or using synthetic methodologies that employ organometallic catalysts [29–34] or oxidant agents [35–37].

Nonetheless, two alternative approaches, both working via one-pot condensation reactions, have been proposed by Wang et al. [38] and by Crawforth et al. [39] to obtain single 1,3-substituted imidazo[1,5-a]pyridine nucleus. The former procedure has been recently employed by us to synthesize tetradentate nitrogen heterocyclic ligands containing two imidazo[1,5-a]pyridine moieties [40]. This simple methodology, however, suffers some limitations such as the availability of poly-aldehydes compatible with the reaction conditions and the impossibility to obtain multiple imidazo[1,5-a]pyridine in *ortho* position on an aromatic ring. In order to bypass such limits, in the present work we adopt the approach reported by Crawforth et al., consisting on a simple one-pot two component condensation involving the reaction of 2-methylaminopyridines with mono carboxylic acid in dehydrating condition to obtain 1-substituted imidazo[1,5-a]pyridines.

Applying this methodology, we synthesized a series of new multiple imidazo[1,5-a]pyridines (Fig. 1) connected by different linkers and succeeded in positioning two imidazo[1,5-a]pyridine in *ortho* position on an aromatic ring, a structural aspect particularly important to ensure a geometry equivalent to the most investigated multi-pyridine ligands largely employed in coordination chemistry [41,42].

Besides these interesting chelating behaviour, the resulting products show interesting optical properties as UV absorber or downshifter[43], as well as good luminescences with moderate quantum yields and large Stokes' shifts. The study of such multiple imidazo[1,5-a]pyridines is a topic that has recently gained attention, due to their structural and tuneable optical behaviour [9,10,44,40].

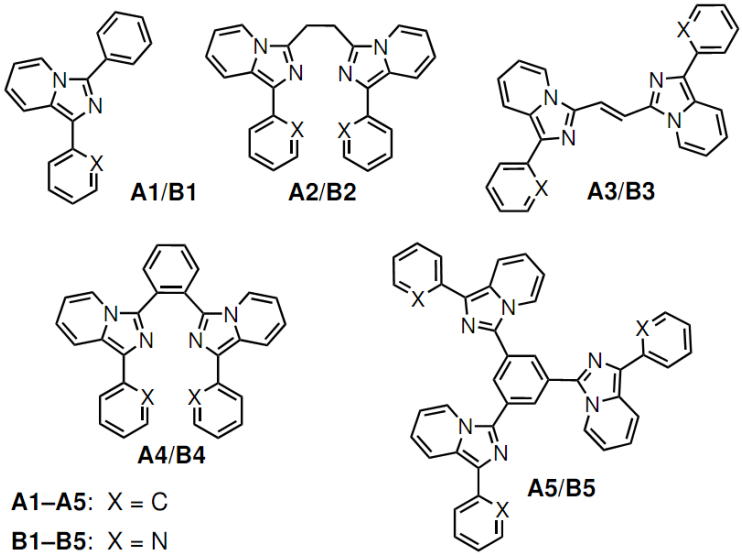

Fig. 1. General structures of studied compounds.

2. Results and Discussion

2.1 Synthesis

This work implements a one-pot procedure first proposed by Crawforth et al. [39] to obtain 1,3-substituted imidazo[1,5-a]pyridines. The original work starts from monocarboxylic acids and 2-methylaminopyridines and uses propylphosphonic anhydride (T3P) in ethyl or *n*-butyl acetate. The present paper extends the previous procedure to a direct double or triple cyclization with two substituted methanamines and different di- or tricarboxylic acids in presence of T3P in *n*-butyl acetate at reflux (Scheme 1).

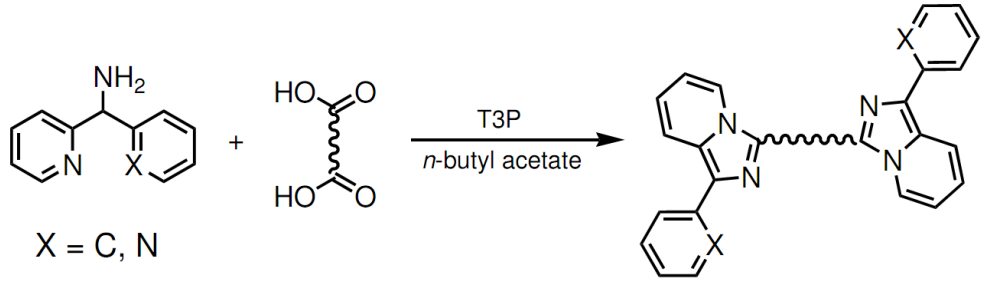

Scheme 1. General synthesis of compounds **A2–5** and **B2–5**.

This approach gives a variety of bis or tris 1-imidazo[1,5-a]pyridine in high yields. As in the case of the monocyclization [39], the reaction tolerates different carboxylic acids and also differently substituted methanamines.

A first cyclization reaction was carried out between phenyl(pyridin-2-yl)methanamine and succinic acid. The product **A2** was recovered as a yellow powder. The same procedure, performed using di(pyridin-2-yl)methanamine, gave the corresponding product which shows pyridine pendant groups (**B2**). Employing phenyl(pyridin-2-yl)methanamine or di(pyridin-2-yl)methanamine and maleic acid we obtained respectively **A3** and **B3**. In both cases, the pure *trans* isomer was obtained, due to great steric hindrance, acidic conditions and high reaction temperature, as previously reported for similar reaction conditions [45]. ^{1}H- and ^{13}C-NMR spectroscopy, X-ray diffraction and TLC analysis confirmed the purity of the *trans* isomers (**A3**, **B3**).

The synthetic versatility of this approach met the challenge of preparing a variety of compounds in a single step, starting from widely available and cheap carboxylic acids. Indeed, using phthalic acid we got two products (**A4** and **B4**) containing double imidazo[1,5-a]pyridine nucleus linked by an aromatic moiety. In this particular case, the alternative approach reported in literature [40] completely fails, leading instead to the isoindole core [46]. For this reason, the method here implemented represents, to the best of our knowledge, the only valid synthetic approach to obtain two imidazo[1,5-a]pyridine in *ortho* position on an aromatic ring. This is a particular important structural aspect because only the *ortho* substitution ensures a geometry equivalent to the most investigate multi-pyridine ligands largely employed in coordination chemistry [47–51].

Finally, involving benzene-1,3,5-tricarboxylic acid, we obtained compounds **A5** and **B5** which have the typical structural motif of multiazine ligands, showing three imidazo[1,5-a]pyridine moieties.

It is noteworthy that using two methanamines, namely phenyl(pyridin-2-yl)methanamine and di(pyridin-2-yl)methanamine, and many different carboxylic acids, it is possible to obtain several imidazo[1,5-a]pyridine derivatives not accessible with the Wang's approach [38] employed in our previous work (Part I) [40]. For instance, all di- and tricarboxylic acids employed in this work (succinic acid for **A2** and **B2**, maleic acid for **A3** and **B3**, phthalic acis for **A4** and **B4**, trimesic acid for **A5** and **B5**) are commercially available and inexpensive conversely to the aldehydic analogous required by the previous approach.

Such new poliazine products show different and tuneable coordination motifs suitable for mono-, di-, and tritopic coordination sites. This molecules can be considered as potential multidentate ligands or precursors for supramolecular design [52,53]. In fact similar multi-imidazo[1,5-a]pyridine have already been employed as ditopical ligand in dinuclear complexes [9,10,44]. Similarly, the imidazo[1,5-a]pyridine core substituted in 1 with a pendant pyridine has been used for coordinating transition metal ions, as in the case of 3-substituted-

1-(pyridin-2-yl)imidazo[1,5-a]pyridine [6–8,12,13]. Furthermore, the phenylimidazole moiety has been adopted as cyclometalating ligand [54–59], likewise the more conventional 2-phenylpyridine.

2.2 Optical properties

The 1,3-substituted imidazo[1,5-a]pyridine nucleus is widely reported in literature for its optical properties [6–8,35,36,60] and it is reasonable to presume that the connection of such systems with different linking units can influence the photophysical features of imidazo[1,5-a]pyridines nucleus [34,61].

Electronic absorption and emission properties of **A2–A5** and **B2–B5** have been investigated and compared with those of **A1** and **B1**, that show a single chromogenic/fluorogenic imidazo[1,5-a]pyridine moiety. The main photophysical parameters recorded in acetonitrile solution are reported in Table 1 while the electronic absorption and emission spectra are depicted in Fig. 2–4. Data acquired in different solvent are included in the Supplementary Information file.

For all the compounds, except **A3** and **B3**, the absorption does not extend over 380 nm. The molar extinction coefficients (ε) are comprised between 10000 and 100000 m^2mol^{-1}. The substitution of benzene rings with pyridines results in a great increase of the extinction coefficients (ε), as evidenced comparing **A1–5** with **B1–5**, with the exception of **A3** and **B3**.

The solvent effects (both solvatochromism and halochromism) on the absorption and emission properties of all the compounds have been evaluated (Fig. 4). Solvent polarity barely influences the absorption and emission spectra of **A1–5** and **B1–5** heterocycles, suggesting low charge transfer character of their ground state. A strong halochromic effect differentiates the absorption properties of the **A** and **B** series (see Fig. 4 and Table S1), with a bathochromic shift for the former and an hypsochromic shift for the latter [14,15].

Under UV-vis excitation, all the products display a fluorescence emission centred at about 455–565 nm (Fig. 3), characterized by quantum yields ranging from 6 to 37%. These values are comparable to the best results reported in literature for imidazo[1,5-a]pyridine based compounds [38,62–64]. In addition, the 1,3-diarylated imidazopyridines display quantum yields that are greatly improved if compared to those of the parent 3-monosubstituted compounds [34–36].

Table 1 Absorption and emission properties of compounds **A1–5** and **B1–5** in CH_3CN solution.

	λ_{abs} (nm)	ε (m^2mol^{-1})	λ_{em} (nm)	Stokes' shift (nm)	ϕ	τ
A1	304	15285	478	174	0.12	5.8
	340sh	9456				
	384sh	3981				
B1	322	24843	460	138	0.18	4.6
	384sh	11258				
A2	305	19541	480	110	0.16	6.8
	370	7612				
B2	284	18249	459	92	0.34	8.5
	332	21176				
	367	20159				
A3	307	18255	491	26	0.10	1.0
	437	27944	524			
	465	22564	565sh			
B3	418	23680	490	25	0.37	1.4
	438	26752	523			
	468	19584	565sh			
A4	302	23452	478	131	0.11	5.9
	347	12203				
B4	300sh	23878	459	100	0.15	5.0
	327	28333				
	359	23513				
A5	302	50282	476	118	0.06	5.0
	358	48219				
B5	329	91474	457	97	0.11	4.0
	360	97333				

All the compounds show wide Stokes' shifts, spanning from 90 to 175 nm; only **A3** and **B3** differ, displaying a shift of about 25 nm. The substitution of the benzene ring with a pyridine greatly increases the quantum yield and causes a blue shift in the emission spectra at about 20 nm, as evidenced comparing **A1–5** with **B1–5**.

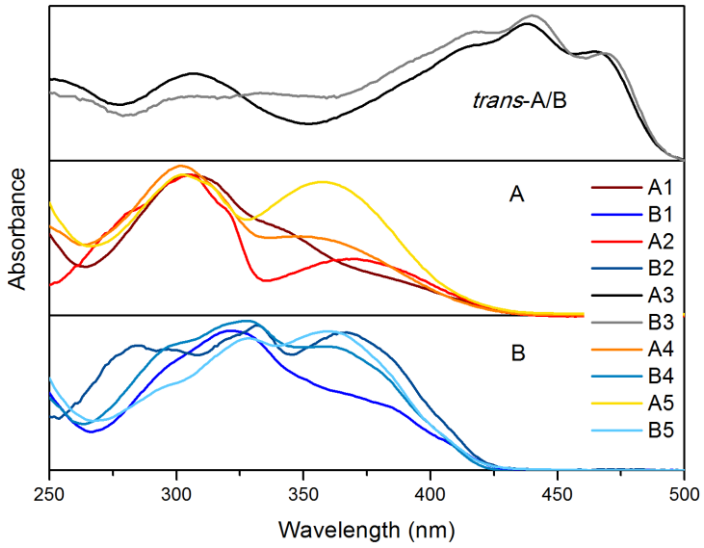

Fig. 2. Experimental electronic absorption spectra in CH_3CN solution.

The absorption properties of **A1**, **A4** and **A5** (as well as **B1**, **B4** and **B5**) show an hyperchromic shift varying the number of chromogenic units bonded to the central aromatic ring; the molar extinction coefficients increase from 11000 m^2mol^{-1} at 384 nm (**A1**), to 23000 m^2mol^{-1} at 359 nm (**A4**), to 97000 m^2mol^{-1} at 360 nm (**A5**). Conversely, increasing the number of fluorogenic units decreases the emission quantum yield i.e. 0.12 for **A1** and 0.06 for **A5** or 0.20 for **B1** and 0.11 for **B5**.

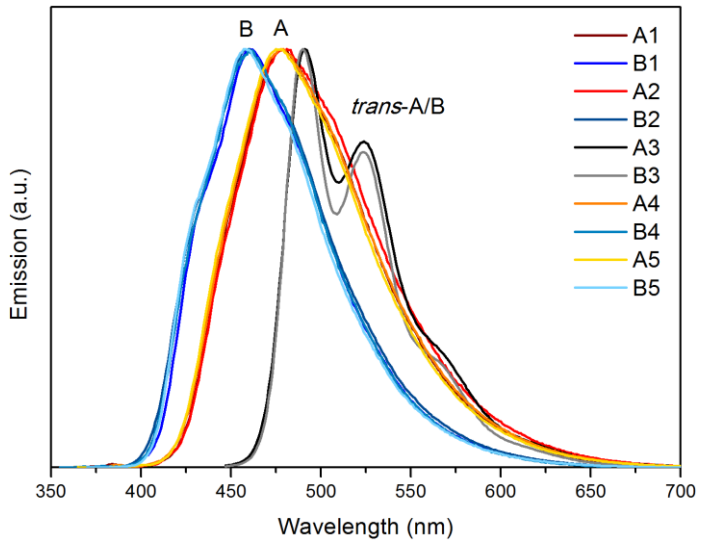

Fig. 3. Experimental emission spectra in CH_3CN solution.

Analogously, the emission properties of **A2**, **A3** and **A4** (or **B2**, **B3** and **B4**) show that the modification of the connection structure between the fluorogenic units influences their photophysical properties [61,65]. In particular, linking two imidazo[1,5-a]pyridine with a *trans*-1,2-ethylene the optical properties dramatically change. Indeed, both **A3** and **B3** display a strong bathochromic effect (80 nm), a reduced Stokes' shift (25 nm), and a short lifetime (lower than 1 ns), if compared to the other imidazo[1,5-

a]pyridines. Moreover, with the *trans*-1,2-ethylene connection there is no difference in absorption and emission properties, between 1-phenyl and 1-pyridil substituted derivative.
A strong halochromic effect differentiates the **A** and **B** series, with a hypsochromic shift for the former and an bathochromic shift for the latter (see Fig. 4, Table S1 and Table S2 for absorption and emission data) [14,15].
All the compounds, with the exception of **A3** and **B3**, show intense absorptions in the near UV, intense emissions in the visible region, large Stokes' shifts and acceptable quantum yields, as required for UV absorption and down-shifting applications.

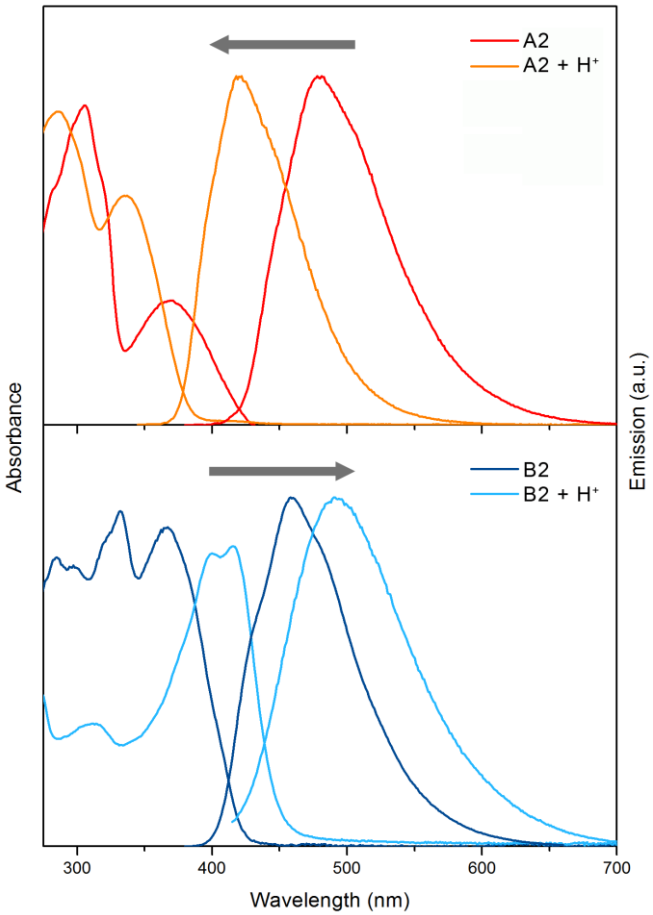

Fig. 4. Experimental absorption and emission spectra of **A2** (top) and **B2** (bottom) in CH_3CN solution prior to (red and blue) and after (orange and light blue) addition of formic acid (1% v/v) to the sample.

2.3 Vibrational characterization

The comparison between FT-IR spectra (Table 2) of pyridil and phenyl derivatives points out some trends. In the couple **A1** and **B1**, there is little changing in frequencies between the two spectra. The most important shift can be seen on the 1595 (**A1**)/1585 (**B1**) cm^{-1} peak and in the low frequency γ(CCC) mode at 493 (**A1**)/479 (**B1**) cm^{-1}, weakened by the nitrogen substitution. Higher differences can be detected in intensities. In the couple **A2** and **B2** there is a clear red shift of many peaks that suggests some different packing into the solid state due to the nitrogen substitution. The peaks at 2960, 2923 and 2855 cm^{-1} $\nu(C–H_{aliph})$, and at 953 (**A2**) or 959 (**B2**) cm^{-1} $\nu(C–C_{aliph})$ confirm the aliphatic nature of the central bond. In the couple **A3** and **B3** the two spectra are quite similar. The appearance of a weak shoulder at about 1630 cm^{-1}, due to alkene C=C double bond stretching, confirms the olefinic nature of the central bond and allows a clear assignation of the peak at 2992 (**A3**)/2994 (**B3**) cm^{-1} to $\nu(C–H_{olef})$. For the couple **A4** and **B4**, the main differences are due to the intensities in the region of C–H bending and ring breathing. **A5** and **B5** derivatives show stronger

differences in intensities, and moderate shifts in peaks in the region of ring deformation modes and of in-plane C–H bending.

Table 2. Vibrational data and comparisons between **1**–**5** phenyl (**A**) and pyridyl (**B**) derivatives. (data reported in cm^{-1}).

1		**2**		**3**		**4**		**5**	
A	**B**	**A**	**B**	**A**	**B**	**A**	**B**	**A**	**B**
1595 m	1585 m	3101 m	3111 m	3126 w	3107 w	3055		3075 w	
1510 m		3054 m	3046 m	3061 w	3041 w	2924 w	2932 w	3025 w	
1480 m		2960/ 2923/ 2855 s		2992 s	2994 s	2853 s	2869 s	3029 w	
1403 m		1598 m	1584 m	1625 m	1628 m	1598 m	1588 m	1591 m	1585 m
1356 m		1514 m	1520 m	1585 m	1598 m	1516 m	1512 m	1515 w	
1302 m		1469 vw	1469 s	1485 vw	1469 s	1490 vw	1473 s	1491 s	1473 s
1248 m		1377 m	1371 m	1326 w		1363 w	1358	1300 s	
1074 m		1260 m	1239 m	1246 m		1316 m		1245 m	
1010 m		1052 m	1058 m	1219 m		1260 m	1246	1040 m	
979 m		953 m	959 m	1131 m	1143 m	1141 w	1141 m	956 m	964 m
948 m		797 m	787 m	1066 m	1073 m	1008		884 m	894 m
788 m	788 s	768 m		1001 m		947 m		792 s	787 s
771 m		417 s	430 s	956 m	963 m	798 m	791 m	768w	
738 m				938 w		770 w		744 m	740 m
691 vs						742 w	736 w	695 m	
613 m	621m					695 m		686 s	
493 m	479 m					423 w	421		

2.4 Crystallografic characterization

Crystals of compounds **A2**, **B2** and **A3** were isolated by slow crystallization and used for the structural characterization. **A2** and **A3** have been crystallized in yellow prisms from dichloromethane added with acetic acid, while **B2** crystals have been obtained from a methanol solution with a very slow evaporation.

Compounds **A2** and **B2** present monoclinic P21/c and C2/c space groups respectively, while **A3** crystallizes in a triclinic P-1 space group. The three compounds are very similar at a molecular level, showing a *trans* configuration around the central C–C double bond of **A3** and a staggered antiperiplanar conformation in the case of **A2** and **B2** (Fig. 5 and Fig. S1), probably due to the big steric hindrance of the substituents. In **A3** the lateral phenyl rings are more coplanar with respect to the others, with a dihedral angle of 2.69(10)° between the two rings. The three compounds are also very similar in the hydrogen bond and the π-π interaction possibilities. This can be observed by the Full Interaction Maps (that show the most probable reciprocal disposition of two functional groups in the space, derived from crystallographic database data) [66] generated with Mercury [67] using the O–H group, the oxygen acceptor and the C(aromatic) probes for checking the hydrogen bond and the π-π donor and acceptor properties (Fig. S3). All the compounds have clearly a propensity to interact with hydrogen bonds to the N-sites of the imidazo[1,5-a]pyridine backbone and with possible hydrophobic interactions to the phenyl rings while the surface (Fig. S3) suggests the presence of weak C–H···O hydrogen interactions with the aromatic C–H bonds. In the crystal packing, these interactions are expressed by different peculiarities that have been analyzed using the Hirshfeld surface approach [68]. The presence of cocrystallized solvent molecules (water for **A3** and **B2** and water and acetic acid molecules in **A2**) can be explained by the aptitude of these organic molecules to form hydrogen bonds. These solvents form chains of hydrogen bonds that propagate along the a axis, surrounded by a channel of organic molecules (Fig. 5, S1 and S2). The walls of these channels are perfectly formed in **A2** (Fig. 5) and **B2** (Fig. S1) that are quite similar in packing, forming a rhomboidal shape, while in A3 the wall of the channels displays two opposite longitudinal fissures extending for the entire length of the channel (Fig. 5). This architecture is stabilized by a series of intermolecular interactions that can be seen into the molecular fingerprint decomposed into its components [69] (Fig. S6, S9 and S12). The principal interactions are the strong O–H···N and the

weaker C–H···O hydrogen bonds with the solvent intercalated molecules (the hydrogen bonds are clearly present in the fingerprint for the typical spikes [70] (Fig. S9 e), less pronounced for the molecule of **A3** than for **A2** due to the greater acidity of the acetic acid respect to water). This tendency is less pronounced in **B2**, where the strong hydrogen bond is the most important interaction. There are also clear contributions from π···π interactions between the imidazo[1,5-a]pyridine rings (visible for the typical blue and red triangles in the shape index curves [71], Fig. S4 d, S7 e-f and S10 e-f) and from C–H···π interactions (especially localized on phenyl groups, as can be seen in the shape index curve for the red circular spots, and clearly present in the fingerprint for the typical lateral wings [71]) that stabilize the organic framework.

The principal difference is due to the presence or the absence of the central double bond, that forces the planarity of the entire molecule as can be observed into the curvedness surface images (Fig. S4 a, S7 a-d and S10 a-b) [68], where blue lines delimitate the surface of interaction between two specific molecules. When the molecule is planar for the double bond, there is a single specific interaction between two entire molecules that cover the face, while in the presence of the single bond a blue line separate the regions of the two imidazo[1,5-a]pyridine rings and two parts of the same face interacts with distinct individuals. This implies the appearance of fissured channels in **A3** and of fully formed channels in the structure of **A2** and **B2**.

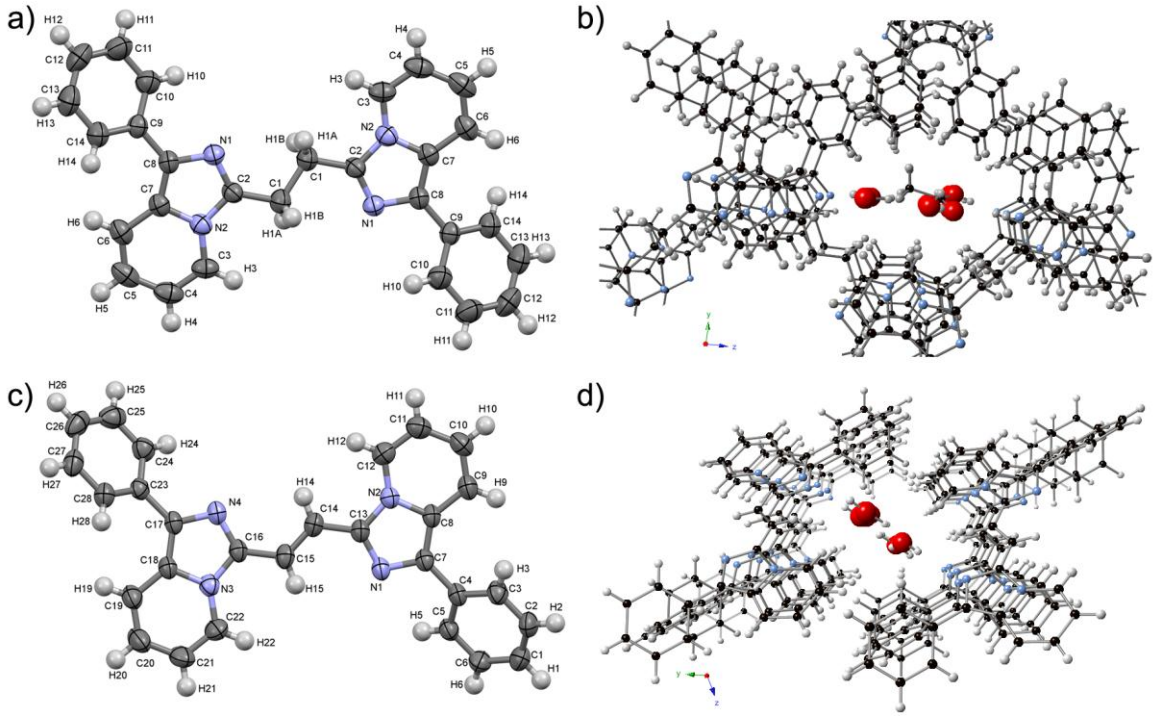

Fig. 5. Molecular structure of **A2** (a) and **A3** (c) with the correspondent crystal packing for **A2** (b) and **A3** (d).

3. Experimental

3.1. General experiments

A1 [18], **B1** [7], phenyl(pyridin-2-yl)methanamine [72–74] and di(pyridin-2-yl)methanamine [75,76] have been synthetized as previously reported.

All solvents and raw materials were used as received from commercial suppliers without further purification. Column chromatography was performed on Sigma Aldrich silica gel 60 (70-230 mesh ASTM). TLC was performed on Fluka silica gel TLC-PET foils GF 254, particle size 25 mm, medium pore diameter 60 A.

^{1}H and ^{13}C NMR spectra were recorded on a JEOL ECP 400 spectrometer (^{1}H NMR operating frequency 400 MHz) with chemical shifts referenced to residual protons in the solvent ($CDCl_3$). The

following abbreviations are used: s (singlet), d (doublet), t (triplet), dd (doublet of doublets), m (multiplet).
UV-Vis absorption spectra were recorded on a Cary60 spectrometer using different solvents in order to investigate the solvatochromic behavior of **A1–5** and **B1–5**. A stock solution (1×10^{-3} M) in dichloromethane was prepared and dilutions (1×10^{-5} M) in dichloromethane, acetonitrile, water were analyzed (or the same solutions acidified at 5 % with formic acid). Photoemission spectra, luminescence lifetimes and quantum yields were acquired with a HORIBA Jobin Yvon IBH Fluorolog-TCSPC spectrofluorometer, equipped with a Quanta-φ integrating sphere. The spectral response was corrected for the spectral sensitivity of the photomultiplier. Luminescence lifetimes were determined by time-correlated single-photon counting; excitation was achieved with nanosecond pulses generated by NanoLED pulsed diodes. Emission-decay data were collected in 2048 channels to 10000 counts in the peak channel and analysed with the software DAS6 (TCSPC decay-analysis software).

3.2. Syntheses

3.2.1 General procedure for bis and tris imidazo[1,5-a]pyridines
The organic acid (2.0 mmol) was added to a solution of phenyl(pyridin-2-yl)methanamine (or di(pyridin-2-yl)methanamine) (4.0 mmol or 6.0 mmol for **A5**, **B5**), in n-butyl acetate (25 mL) at rt. The resulting slurry was added with 7.5 mL of T3P (propylphosphonic anhydride Aldrich 50% solution in EtOAc), the solution was stirred at rt for 1h, before being heated at reflux for 16h. The reaction mixture was cooled to room temperature and the butyl acetate was removed by evaporation under vacuum. The solid was dissolved in saturated sodium carbonate solution and the mixture extracted with CH_2Cl_2 (3 x 10 mL). The organic layer was separated, dried and the solvent evaporated under vacuum. The formed solid was washed several times with diethyl ether and dried under vacuum obtaining the product as a yellow powder. For **A2**, **A3**, **B2** and **B3** the residue was purified by flash chromatography over silica gel (CH_2Cl_2/CH_3OH 98:2 for **A2**, **A3** and 96:4 for **B2**, **B3**).

3.2.2 1-phenyl-3-(2-(1-phenylH-imidazo[1,5-a]pyridin-3-yl)ethyl)H-imidazo[1,5-a]pyridine (**A2**).
Yields 98.0, 0.814 g. MS (ESI): *m/z* $C_{28}H_{22}N_4$ 415.19 [$(M + H^+)$]. ^{1}H NMR ($CDCl_3$, 400 MHz): δ = 7.84 (4H, d, J = 7.8 Hz), 7.74 (2H, d, J = 6.8 Hz), 7.68 (2H, d, J = 9.2 Hz), 7.45 (4H, t, J = 7.7 Hz), 7.29 (2H, t, J = 7.5 Hz), 6.67 (2H, dd), 6.45 (2H, t, J = 6.8 Hz), 3.73 (4H, s) ppm. ^{13}C NMR ($CDCl_3$, 100 MHz): δ = 136.9, 133.8, 129.2, 128.9, 126.8, 126.7, 121.7, 119.4, 118.7, 113.5, 24.6 ppm

3.2.3 1-phenyl-3-((1E)-2-(1-phenylH-imidazo[1,5-a]pyridin-3-yl)vinyl)H-imidazo[1,5-a]pyridine (**A3**).
Yields 72.4%, 0.598 g. MS (ESI): *m/z* $C_{28}H_{20}N_4$ 413.18 [$(M + H^+)$]. ^{1}H NMR ($CDCl_3$, 400 MHz): δ = 8.24 (2H, d, J = 7.0 Hz), 7.96 (2H, s), 7.94 (4H, d, J = 7.8 Hz), 7.81 (2H, d, J = 9.2 Hz), 7.49 (4H, t, J = 7.8 Hz), 7.33 (2H, t, J = 7.3 Hz), 6.83 (2H, dd), 6.71 (2H, dd) ppm. ^{13}C NMR ($CDCl_3$, 100 MHz): δ = 136.6, 134.8, 133.3, 128.9, 128.1, 127.1, 127.0, 121.7, 120.3, 119.3, 113.8, 113.0 ppm.

3.2.4 1-phenyl-3-(2-(1-phenylH-imidazo[1,5-a]pyridin-3-yl)phenyl)H-imidazo[1,5-a]pyridine (**A4**).
Yields 24.0%, 0.222 g. MS (ESI): *m/z* $C_{32}H_{22}N_4$ 463.19 [$(M + H^+)$]. ^{1}H NMR ($CDCl_3$, 400 MHz): δ = 7.96 (2H, dd), 7.80 (4H, d, J = 8.0 Hz), 7.67 (2H, dd), 7.55 (2H, d, J = 9.2 Hz), 7.44 (6H, m), 7.28 (2H, t, J = 7.4 Hz), 6.51 (2H, dd), 6.14 (2H, t, J = 7.3 Hz) ppm. ^{13}C NMR ($CDCl_3$, 100 MHz): δ = 136.7, 135.1, 132.4, 132.2, 129.9, 129.6, 128.8, 127.5, 126.8, 126.6, 121.5, 119.9, 118.1, 112.5 ppm.

3.2.5 3-(3,5-bis(1-phenylH-imidazo[1,5-a]pyridin-3-yl)phenyl)-1-phenylH-imidazo[1,5-a]pyridine (**A5**).
Yields 88.1%, 1.15 g. MS (ESI): *m/z* $C_{45}H_{30}N_6$ 655.26 [$(M + H^+)$]. ^{1}H NMR ($CDCl_3$, 400 MHz): δ = 8.50 (3H, d, J = 6.9 Hz), 7.44 (3H, s), 7.96 (6H, d, J = 7.2 Hz), 7.98 (3H, d, J = 9.4 Hz), 7.48 (6H, t, J = 7.7 Hz), 7.32 (3H, t, J = 7.4 Hz), 6.87 (3H, dd), 6.69 (3H, t, J = 6.8 Hz) ppm. ^{13}C NMR ($CDCl_3$, 100 MHz): δ = 136.7, 134.5, 132.3, 131.8, 128.9, 128.2, 128.0, 127.0, 127.0, 122.2, 120.5, 119.3, 114.3 ppm.

3.2.6 1-(pyridin-2-yl)-3-(2-(1-(pyridin-2-yl)H-imidazo[1,5-a]pyridin-3-yl)ethyl)H-imidazo[1,5-a]pyridine (**B2**).

Yields 56.5%, 0.471 g. MS (ESI): *m/z* $C_{26}H_{20}N_6$ 417.18 [(M + H^+)]. ^{1}H NMR ($CDCl_3$, 400 MHz): δ =8.60 (2H, d, J = 5.0 Hz), 8.50 (2H, d, J = 9.2 Hz), 8.10 (2H, d, J = 8.0 Hz), 7.70 (4H, m), 7.06 (2H, dd), 6.79 (2H, dd), 6.51 (2H, t, J = 7.0 Hz), 3.67 (4H, s) ppm. ^{13}C NMR ($CDCl_3$, 100 MHz): δ = 156.1, 149.2, 137.6, 136.3, 129.5, 129.1, 121.3, 121.0, 120.5, 120.3, 119.7, 113.4, 24.8 ppm

3.2.7 1-(pyridin-2-yl)-3-((1E)-2-(1-(pyridin-2-yl)H-imidazo[1,5-a]pyridin-3-yl)vinyl)H-imidazo[1,5-a]pyridine (**B3**).

Yields 55.1%, 0.458 g. MS (ESI): *m/z* $C_{26}H_{18}N_6$ 415.67 [(M + H^+)]. ^{1}H NMR ($CDCl_3$, 400 MHz): δ = 8.66 (4H, m), 8.41 (2H, d, J = 7.0 Hz), 8.36 (2H, d, J = 8.0 Hz), 7.15 (2H, s), 7.78 (2H, t, J = 8.0 Hz), 7.15 (2H, m), 7.01 (2H, m), 6.85 (2H, t, J = 7.0) ppm. ^{13}C NMR ($CDCl_3$, 100 MHz): δ = 153.5, 148.8, 136.9, 136.4, 130.7, 122.5, 122.0, 121.8, 121.1, 120.5, 115.1, 113.4 ppm.

3.2.8 1-(pyridin-2-yl)-3-(2-(1-(pyridin-2-yl)H-imidazo[1,5-a]pyridin-3-yl)phenyl)H-imidazo[1,5-a]pyridine (**B4**).

Yields 99.0%, 0.921 g. MS (ESI): *m/z* $C_{30}H_{20}N_6$ 465.18 [(M + H^+)]. ^{1}H NMR ($CDCl_3$, 400 MHz): δ = 8.55 (2H, d, J = 4.8 Hz), 8.41 (2H, d, J = 9.0 Hz), 8.02 (2H, d, J = 8.0 Hz), 7.94 (2H, m), 7.65 (4H, m), 7.57 (2H, d, J = 7.2 Hz), 7.04 (2H, m), 7.67 (2H, m), 6.24 (2H, t, J = 6.8) ppm. ^{13}C NMR ($CDCl_3$, 100 MHz): δ = 155.0, 149.0, 136.6, 136.3, 132.1, 130.8, 130.0, 129.9, 129.8, 121.4, 121.3, 120.9, 120.5, 120.0, 113.4 ppm.

3.2.9 3-(3,5-bis(1-(pyridin-2-yl)H-imidazo[1,5-a]pyridin-3-yl)phenyl)-1-(pyridin-2-yl)H-imidazo[1,5-a]pyridine (**B5**).

Yields 71.8%, 0.945 g. MS (ESI): *m/z* $C_{42}H_{27}N_9$ 658.25 [(M + H^+)]. ^{1}H NMR ($CDCl_3$, 400 MHz): δ = 8.77 (3H, d, J = 9.1 Hz), 8.65 (3H, d, J = 4.1 Hz), 8.44 (6H, m), 8.28 (3H, d, J = 8.0 Hz), 7.74 (3H, t, J = 7.8 Hz), 7.12 (3H, dd), 6.99 (3H, dd), 6.74 (3H, t, J = 6.5 Hz) ppm. ^{13}C NMR ($CDCl_3$, 100 MHz): δ = 154.8, 148.8, 136.9, 136.6, 132.1, 131.1, 130.9, 128.0, 122.1, 121.8, 121.6, 120.8, 120.7, 114.7 ppm.

4. Conclusions

In this paper we presented a new series of poly 1,3-substituted imidazo[1,5-a]pyridines obtained by means of one-pot multiple cyclizations of two different methanamine with several stable, inexpensive and largely available carboxylic acids. Furthermore, to the best of our knowledge, two imidazo[1,5-a]pyridines in ortho position on an aromatic ring have been synthesized for the first time.

All the compounds show interesting photophysical properties, with a wide variety of fluorescent emissions (460–520 nm), large Stokes' shifts and, depending on the chemical structure of the linking units between the imidazo[1,5-a]pyridine moieties, fluorescence quantum yields (Φ) that span from 10 % to 40 %. The crystal structures of **A2**, **A3** and **B2** have also been solved, confirming in particular the complete *cis-trans* conversion of the maleic acid derivatives.

The present work allows extending the previously reported class of fluorescent multiazine derivatives, easily tuneable and potentially interesting for applications in the fields of DSCs, LECs and NLO. The negligible overlap between absorption and emission spectra provides an interesting low cost candidate for UV absorption and down-shifting applications.

Good reaction yields, high stability and accessibility of reagents, absence of catalysts make this synthetic approach useful for a systematic screening and up-scaling of a large number of compounds. On the basis of this promising one-pot multiple cyclization synthetic approach, further studies on the development of a diversity-oriented introduction of different linking units into poly imidazo[1,5-a]pyridine skeleton on the photophysical features are in progress in our laboratories.

Acknowledgements

Authors gratefully acknowledge financial support from University of Torino (Ricerca Locale ex-60%, Bando 2016).

Notes

CCDCs 1536537-1536539 contain the supplementary crystallographic data for this paper. These data can be obtained free of charge from The Cambridge Crystallographic Data Centre via www.ccdc.cam.ac.uk/data_request/cif.

References

[1] M. Alcarazo, S.J. Roseblade, A.R. Cowley, R. Fernandez, J.M. Brown, J.M. Lassaletta, J. Am. Chem. Soc. 127 (2005) 3290–3291.
[2] C. Burstein, C.W. Lehmann, F. Glorius, Tetrahedron 61 (2005) 6207–6217.
[3] F.E. Hahn, Angew. Chem.-Int. Ed. 45 (2006) 1348–1352.
[4] S.J. Roseblade, A. Ros, D. Monge, M. Alcarazo, E. Alvarez, J.M. Lassaletta, R. Fernandez, Organometallics 26 (2007) 2570–2578.
[5] M.D. Weber, C. Garino, G. Volpi, E. Casamassa, M. Milanesio, C. Barolo, R.D. Costa, Dalton Trans. 45 (2016) 8984–8993.
[6] G. Volpi, C. Garino, L. Salassa, J. Fiedler, K.I. Hardcastle, R. Gobetto, C. Nervi, Chem.- Eur. J. 15 (2009) 6415–6427.
[7] L. Salassa, C. Garino, A. Albertino, G. Volpi, C. Nervi, R. Gobetto, K.I. Hardcastle, Organometallics 27 (2008) 1427–1435.
[8] C. Garino, T. Ruiu, L. Salassa, A. Albertino, G. Volpi, C. Nervi, R. Gobetto, K.I. Hardcastle, Eur. J. Inorg. Chem. (2008) 3587–3591.
[9] N. Kundu, M. Maity, P.B. Chatterjee, S.J. Teat, A. Endo, M. Chaudhury, J. Am. Chem. Soc. 133 (2011) 20104–20107.
[10] N. Kundu, S.M.T. Abtab, S. Kundu, A. Endo, S.J. Teat, M. Chaudhury, Inorg. Chem. 51 (2012) 2652–2661.
[11] Y. Chen, L. Li, Y. Cao, J. Wu, Q. Gao, Y. Li, H. Hu, W. Liu, Y. Liu, Z. Kang, J. Li, Crystengcomm 15 (2013) 2675–2681.
[12] G.A. Ardizzoia, S. Brenna, S. Durini, B. Therrien, Polyhedron 90 (2015) 214–220.
[13] G.A. Ardizzoia, S. Brenna, S. Durini, B. Therrien, M. Veronelli, Eur. J. Inorg. Chem. (2014) 4310–4319.
[14] J.T. Hutt, J. Jo, A. Olasz, C.-H. Chen, D. Lee, Z.D. Aron, Org. Lett. 14 (2012) 3162–3165.
[15] X. Zhang, G.-J. Song, X.-J. Cao, J.-T. Liu, M.-Y. Chen, X.-Q. Cao, B.-X. Zhao, Rsc Adv. 5 (2015) 89827–89832.
[16] G.-J. Song, S.-Y. Bai, X. Dai, X.-Q. Cao, B.-X. Zhao, Rsc Adv. 6 (2016) 41317–41322.
[17] J. Hu, Y. Li, Y. Wu, W. Liu, Y. Wang, Y. Li, Chem. Lett. 44 (2015) 645–647.
[18] G. Volpi, G. Magnano, I. Benesperi, D. Saccone, E. Priola, V. Gianotti, M. Milanesio, E. Conterosito, C. Barolo, G. Viscardi, Dyes Pigments 137 (2017) 152–164.
[19] D. Kim, L.P. Wang, J.J. Hale, C.L. Lynch, R.J. Budhu, M. MacCross, S.G. Mills, L. Malkowitz, S.L. Gould, J.A. DeMartino, M.S. Springer, D. Hazuda, M. Miller, J. Kessler, R.C. Hrin, G. Carver, A. Carella, K. Henry, J. Lineberger, W.A. Schleif, E.A. Emini, Bioorg. Med. Chem. Lett. 15 (2005) 2129–2134.
[20] D. Davey, P.W. Erhardt, W.C. Lumma, J. Wiggins, M. Sullivan, D. Pang, E. Cantor, J. Med. Chem. 30 (1987) 1337–1342.
[21] L.J. Browne, C. Gude, H. Rodriguez, R.E. Steele, A. Bhatnager, J. Med. Chem. 34 (1991) 725–736.
[22] N.F. Ford, L.J. Browne, T. Campbell, C. Gemenden, R. Goldstein, C. Gude, J.W.F. Wasley, J. Med. Chem. 28 (1985) 164–170.
[23] B.P. Fauber, A. Gobbi, K. Robarge, A. Zhou, A. Barnard, J. Cao, Y. Deng, C. Eidenschenk, C. Everett, A. Ganguli, J. Hawkins, A.R. Johnson, H. La, M. Norman, G. Salmon, S. Summerhill, W. Ouyang, W. Tang, H. Wong, Bioorg. Med. Chem. Lett. 25 (2015) 2907–2912.

[24] R. Nirogi, A.R. Mohammed, A.K. Shinde, N. Bogaraju, S.R. Gagginapalli, S.R. Ravella, L. Kota, G. Bhyrapuneni, N.R. Muddana, V. Benade, R.C. Palacharla, P. Jayarajan, R. Subramanian, V.K. Goyal, Eur. J. Med. Chem. 103 (2015) 289–301.
[25] M. Roy, B.V.S.K. Chakravarthi, C. Jayabaskaran, A.A. Karande, A.R. Chakravarty, Dalton Trans. 40 (2011) 4855–4864.
[26] J.D. Bower, G.R. Ramage, J. Chem. Soc. Resumed (1955) 2834–2837.
[27] H. Zimmer, D.G. Glasgow, M. McClanahan, T. Novinson, Tetrahedron Lett. 9 (1968) 2805–2807.
[28] G. Pelletier, A.B. Charette, Org. Lett. 15 (2013) 2290–2293.
[29] H. Wang, W. Xu, Z. Wang, L. Yu, K. Xu, J. Org. Chem. 80 (2015) 2431–2435.
[30] A. Joshi, D.C. Mohan, S. Adimurthy, Org. Lett. 18 (2016) 464–467.
[31] H.T.H. Nguyen, O.T.K. Nguyen, T. Truong, N.T.S. Phan, Rsc Adv. 6 (2016) 36039–36049.
[32] H. Wang, W. Xu, L. Xin, W. Liu, Z. Wang, K. Xu, J. Org. Chem. 81 (2016) 3681–3687.
[33] A. Moulin, S. Garcia, J. Martinez, J.-A. Fehrentz, Synth.-Stuttg. (2007) 2667–2673.
[34] E. Yamaguchi, F. Shibahara, T. Murai, J. Org. Chem. 76 (2011) 6146–6158.
[35] F. Shibahara, R. Sugiura, E. Yamaguchi, A. Kitagawa, T. Murai, J. Org. Chem. 74 (2009) 3566–3568.
[36] F. Shibahara, E. Yamaguchi, A. Kitagawa, A. Imai, T. Murai, Tetrahedron 65 (2009) 5062–5073.
[37] F. Shibahara, A. Kitagawa, E. Yamaguchi, T. Murai, Org. Lett. 8 (2006) 5621–5624.
[38] J. Wang, L. Dyers, R. Mason, P. Amoyaw, X. Bu, J. Org. Chem. 70 (2005) 2353–2356.
[39] J.M. Crawforth, M. Paoletti, Tetrahedron Lett. 50 (2009) 4916–4918.
[40] G. Volpi, C. Garino, E. Conterosito, C. Barolo, R. Gobetto, G. Viscardi, Dyes Pigments 128 (2016) 96–100.
[41] A.O. Adeloye, P.A. Ajibade, Molecules 19 (2014) 12421–12460.
[42] D. Saccone, C. Magistris, N. Barbero, P. Quagliotto, C. Barolo, G. Viscardi, Materials 9 (2016) 137.
[43] E. Conterosito, I. Benesperi, V. Toson, D. Saccone, N. Barbero, L. Palin, C. Barolo, V. Gianotti, M. Milanesio, Chemsuschem 9 (2016) 1279–1289.
[44] A.L. Guckian, M. Doering, M. Ciesielski, O. Walter, J. Hjelm, N.M. O'Boyle, W. Henry, W.R. Browne, J.J. McGarvey, J.G. Vos, Dalton Trans. (2004) 3943–3949.
[45] M. Baag, A. Kar, N.P. Argade, Tetrahedron 59 (2003) 6489–6492.
[46] T. Do Minh, A.L. Johnson, J.E. Jones, P.P. Senise, J. Org. Chem. 42 (1977) 4217–4221.
[47] A. Abbotto, F. Sauvage, C. Barolo, F. De Angelis, S. Fantacci, M. Graetzel, N. Manfredi, C. Marinzi, M.K. Nazeeruddin, Dalton Trans. 40 (2011) 234–242.
[48] C. Barolo, M.K. Nazeeruddin, S. Fantacci, D. Di Censo, P. Comte, P. Liska, G. Viscardi, P. Quagliotto, F. De Angelis, S. Ito, M. Gratzel, Inorg. Chem. 45 (2006) 4642–4653.
[49] C. Barolo, J.H. Yum, E. Artuso, N. Barbero, D. Di Censo, M.G. Lobello, S. Fantacci, F. De Angelis, M. Gratzel, M.K. Nazeeruddin, G. Viscardi, Chemsuschem 6 (2013) 2170–2180.
[50] T. Renouard, R.A. Fallahpour, M.K. Nazeeruddin, R. Humphry-Baker, S.I. Gorelsky, A.B.P. Lever, M. Gratzel, Inorg. Chem. 41 (2002) 367–378.
[51] T. Renouard, M. Gratzel, Tetrahedron 57 (2001) 8145–8150.
[52] C. Seward, J. Pang, S. Wang, Eur. J. Inorg. Chem. (2002) 1390–1399.
[53] R. Tan, Z.-B. Wang, Y. Li, D.J. Kozera, Z.-H. Lu, D. Song, Inorg. Chem. 51 (2012) 7039–7049.
[54] E. Baranoff, S. Fantacci, F. De Angelis, X.X. Zhang, R. Scopelliti, M. Gratzel, M.K. Nazeeruddin, Inorg. Chem. 50 (2011) 451–462.
[55] A. Herbst, C. Bronner, P. Dechambenoit, O.S. Wenger, Organometallics 32 (2013) 1807–1814.
[56] A.Y.Y. Tam, D.P.K. Tsang, M.Y. Chan, N.Y. Zhu, V.W.W. Yam, Chem. Commun. 47 (2011) 3383–3385.
[57] W.H. Wu, J.Z. Zhao, H.M. Guo, J.F. Sun, S.M. Ji, Z.L. Wang, Chem.- Eur. J. 18 (2012) 1961–1968.
[58] W.W. Yang, Y.W. Zhong, S. Yoshikawa, J.Y. Shao, S. Masaoka, K. Sakai, J.N. Yao, M. Haga, Inorg. Chem. 51 (2012) 890–899.
[59] G.S. Yellol, A. Donaire, J.G. Yellol, V. Vasylyeva, C. Janiak, J. Ruiz, Chem. Commun. 49 (2013) 11533–11535.
[60] A.M. Blanco-Rodríguez, H. Kvapilova, J. Sykora, M. Towrie, C. Nervi, G. Volpi, S. Zalis, A. Vlcek, J. Am. Chem. Soc. 136 (2014) 5963–5973.
[61] E. Yamaguchi, F. Shibahara, T. Murai, Chem. Lett. 40 (2011) 939–940.
[62] S.A. Siddiqui, T.M. Potewar, R.J. Lahoti, K.V. Srinivasan, Synth.-Stuttg. (2006) 2849–2854.
[63] J. Wang, R. Mason, D. VanDerveer, K. Feng, X.R. Bu, J. Org. Chem. 68 (2003) 5415–5418.
[64] A. Rahmati, K. Zahra, Int. J. Org. Chem. 01 (2011) 15–19.

[65] E. Yamaguchi, F. Shibahara, T. Murai, J. Org. Chem. 76 (2011) 6146–6158.
[66] P.A. Wood, T.S.G. Olsson, J.C. Cole, S.J. Cottrell, N. Feeder, P.T.A. Galek, C.R. Groom, E. Pidcock, Crystengcomm 15 (2013) 65–72.
[67] C.F. Macrae, I.J. Bruno, J.A. Chisholm, P.R. Edgington, P. McCabe, E. Pidcock, L. Rodriguez-Monge, R. Taylor, J. van de Streek, P.A. Wood, J. Appl. Crystallogr. 41 (2008) 466–470.
[68] M.A. Spackman, D. Jayatilaka, Crystengcomm 11 (2009) 19–32.
[69] M.A. Spackman, J.J. McKinnon, Crystengcomm 4 (2002) 378–392.
[70] H.F. Clausen, M.S. Chevallier, M.A. Spackman, B.B. Iversen, New J. Chem. 34 (2010) 193–199.
[71] J.J. McKinnon, M.A. Spackman, A.S. Mitchell, Acta Crystallogr. Sect. B-Struct. Sci. 60 (2004) 627–668.
[72] D. Olbert, H. Görls, D. Conrad, M. Westerhausen, Eur. J. Inorg. Chem. 2010 (2010) 1791–1797.
[73] D.V. Griffiths, Y.-K. Cheong, P. Duncanson, M. Motevalli, Dalton Trans. 40 (2011) 10215–10228.
[74] H.S. Jena, V. Manivannan, Inorganica Chim. Acta 390 (2012) 154–162.
[75] C. Najera, J. Gil-Molto, S. Karlstrom, L.R. Falvello, Org. Lett. 5 (2003) 1451–1454.
[76] J. Chang, S. Plummer, E.S.F. Berman, D. Striplin, D. Blauch, Inorg. Chem. 43 (2004) 1735–1742.